



**Discover Generics**

Cost-Effective CT & MRI Contrast Agents

**FRESENIUS  
KABI**

[WATCH VIDEO](#)

**AJNR**

**Predicting Drug Treatment Outcomes in  
Childrens with Tuberous Sclerosis Complex–  
Related Epilepsy: A Clinical Radiomics Study**

Z. Hu, D. Jiang, X. Zhao, J. Yang, D. Liang, H. Wang, C.  
Zhao and J. Liao

This information is current as  
of June 21, 2025.

*AJNR Am J Neuroradiol* published online 22 June 2023  
<http://www.ajnr.org/content/early/2023/06/22/ajnr.A7911>

# Predicting Drug Treatment Outcomes in Childrens with Tuberous Sclerosis Complex–Related Epilepsy: A Clinical Radiomics Study

 Z. Hu,  D. Jiang,  X. Zhao,  J. Yang,  D. Liang,  H. Wang,  C. Zhao, and  J. Liao



## ABSTRACT

**BACKGROUND AND PURPOSE:** Highly predictive markers of drug treatment outcomes of tuberous sclerosis complex–related epilepsy are a key unmet clinical need. The objective of this study was to identify meaningful clinical and radiomic predictors of outcomes of epilepsy drug treatment in patients with tuberous sclerosis complex.

**MATERIALS AND METHODS:** A total of 105 children with tuberous sclerosis complex–related epilepsy were enrolled in this retrospective study. The pretreatment baseline predictors that were used to predict drug treatment outcomes included patient demographic and clinical information, gene data, electroencephalogram data, and radiomic features that were extracted from pretreatment MR imaging scans. The Spearman correlation coefficient and least absolute shrinkage and selection operator were calculated to select the most relevant features for the drug treatment outcome to build a comprehensive model with radiomic and clinical features for clinical application.

**RESULTS:** Four MR imaging–based radiomic features and 5 key clinical features were selected to predict the drug treatment outcome. Good discriminative performances were achieved in testing cohorts (area under the curve = 0.85, accuracy = 80.0%, sensitivity = 0.75, and specificity = 0.83) for the epilepsy drug treatment outcome. The model of radiomic and clinical features resulted in favorable calibration curves in all cohorts.

**CONCLUSIONS:** Our results suggested that the radiomic and clinical features model may predict the epilepsy drug treatment outcome. Age of onset, infantile spasms, antiseizure medication numbers, epileptiform discharge in left parieto-occipital area of electroencephalography, and gene mutation type are the key clinical factors to predict the epilepsy drug treatment outcome. The texture and first-order statistic features are the most valuable radiomic features for predicting drug treatment outcomes.

**ABBREVIATIONS:** ASM = antiseizure medication; AUC = area under the receiver operating curve; EEG = electroencephalography; GLCM = gray-level co-occurrence matrix; GLDM = gray-level dependence matrix; GLRLM = gray-level run-length matrix; GLSZM = gray-level size zone matrix; LASSO = least absolute shrinkage and selection operator; TSC = tuberous sclerosis complex

**T**uberous sclerosis complex (TSC) is a rare autosomal dominant disorder caused by loss-of-function mutations of the *TSC1* or *TSC2* genes, which can affect multiple organ systems<sup>1</sup>

and is frequently associated with tumors of the brain, skin, heart, lungs and kidneys, seizures, and TSC-associated neuropsychiatric disorders, including autism spectrum disorder and cognitive disability.<sup>2</sup> Epilepsy is the most common and clinically challenging symptom of TSC, affecting approximately 85% of patients,<sup>3,4</sup> of which nearly two-thirds have the first seizure in the first year of life.<sup>5,6</sup>

The goal of treatment in TSC is to prevent or control seizures as soon as possible after TSC diagnosis, which will improve cognitive neurodevelopment and enhance the quality of life.<sup>3</sup> The


Received July 31, 2022; accepted after revision May 22, 2023.

From the Departments of Neurology (Z.H., X.Z., J.L.) and Radiology (C.Z.), Shenzhen Children's Hospital, Shenzhen, China; Research Centre for Medical AI (D.J., J.Y., D.L.) and Paul C. Lauterbur Research Center for Biomedical Imaging (D.L., H.W.), Shenzhen Institutes of Advanced Technology, Chinese Academy of Sciences, Shenzhen, Guangdong, China; and Shenzhen College of Advanced Technology (D.J., J.Y., D.L.), University of Chinese Academy of Sciences, Shenzhen, Guangdong, China.

Zhanqi Hu, Dian Jiang, and Xia Zhao contributed equally to this study and are co-first authors.

Some of the work was partially supported by the Sanming Project of Medicine in Shenzhen (SZSM201812005), Shenzhen Key Medical Discipline Construction Fund (No.SZXK033), Shenzhen Fund for Guangdong Provincial High-Level Clinical Key Specialties (No.SZGSP012), Pearl River Talent Recruitment Program of Guangdong Province (2019QN01Y986), Shenzhen Science and Technology Program (JCYJ20210324115810030), National Natural Science Foundation of China (61871373, 81729003, and 81901736), and Shenzhen Fundamental Research Program (JCYJ2018 0228175428243).

Please address correspondence to Jianxiang Liao, MD, Department of Neurology, Shenzhen Children's Hospital, 7019, Yitian Rd, Shenzhen 518038, China; e-mail: liaojianxiang@vip.sina.com

 Indicates open access to non-subscribers at [www.ajnr.org](http://www.ajnr.org)

 Indicates article with online supplemental data.

<http://dx.doi.org/10.3174/ajnr.A7911>

classic treatment for epilepsy is antiseizure medication (ASM).<sup>7</sup> However, >50% of patients with TSC will develop drug-resistant epilepsy,<sup>8,9</sup> and diagnosing it may take a long time.<sup>10</sup> Therefore, there is an urgent need to investigate the predictive biomarkers for the effectiveness of ASM treatment for patients with epilepsy.

Nervous system manifestations can be observed in almost all cases of TSC, and MR imaging is a technique used routinely to diagnose TSC.<sup>11</sup> Cortical tubers are major TSC-related brain manifestations, which show abnormal high or low signals in FLAIR sequences.<sup>12</sup> In addition, FLAIR imaging is widely used to study the epileptogenic zone<sup>13</sup> and epilepsy mechanism of TSC.<sup>14</sup> Jesmanas et al<sup>9</sup> reported that MR imaging-defined tuber types were found to be associated with early seizure onset in TSC. In addition, lesion location and type of information features in MR imaging have been shown to be associated with the outcomes of epilepsy drug treatment.<sup>10</sup> However, the features of MR imaging were typically extracted manually, and the description of these features was usually qualitative, subjective, and nonspecific.

Radiomics is an emerging research branch in the field of medical imaging, which aims to extract mineable high-dimensional data from clinical images.<sup>15,16</sup> Radiomics capture tissue and lesion characteristics, such as heterogeneity, texture, and shape and can be used alone or in combination with demographic, histologic, genomic, or proteomic data to solve clinical problems.<sup>17</sup> Radiomic analyses have been successfully applied to predict the type of tumor-related epilepsy or epilepsy presentation<sup>18-22</sup> and treatment outcomes for cancer.<sup>23-27</sup> Thus, a noninvasive biomarker based on radiomic analyses that can predict the drug treatment outcome in patients with TSC would be valuable.

In this study, we used FLAIR scans to extract radiomic features including shape, first-order statistics, and textural features that are associated with the drug treatment outcome in patients with TSC. Moreover, we constructed a machine learning model to investigate how accurately we can predict the drug treatment outcome in patients with TSC using radiomic and clinical information.

## MATERIALS AND METHODS

### Patients

A total of 105 patients with TSC at Shenzhen Children's Hospital between January 2013 and September 2018 were consecutively enrolled in this retrospective study, and informed consent was obtained from all patients before the study. The protocols were approved by the Ethics Committee of Shenzhen Institutes of Advanced Technology, Chinese Academy of Sciences. We included patients who met the following criteria: 1) They had undergone FLAIR MR imaging before ASM treatment, 2) electroencephalography (EEG) was recorded on admission or as an outpatient, 3) they had ASM treatment for at least 1 year, and 4) the ages at MR imaging were younger than 6 months.

Drug treatment outcome was defined according to the Gül Mert et al<sup>6</sup> and was recorded as controlled or uncontrolled. Patients were considered as controlled if they had not had clinical seizures for at least 1 year. Uncontrolled patients had at least 1 seizure in the past year. Data were randomly split into a training data set ( $n = 75$ ) and an independent test data set ( $n = 30$ ). We

used stratified random sampling to ensure the same class ratios for every set. There was no patient overlap between the training and test sets. The training data set was used to derive clinical and radiomic predictors of epilepsy; then, the classification performance of these predictors was internally validated on the test data set.

Data of 59 routine clinical variables were collected, including patient information, such as sex, age, typical symptoms of TSC, and examination results, as well as *TSC1* and *TSC2* gene test results and EEG features and so forth. This study further used the clinical and MR imaging data of all enrolled cases. The flow chart of the study is illustrated in Fig 1.

### Image Acquisition

All MR imaging examinations were performed using a Magnetom Trio 3T scanner (Siemens) with an 8-channel receive-only head coil acquisition. The FLAIR parameters were as follows: TR = 9000 ms, TE = 132 ms, TI = 2600 ms, flip angle = 150°, FOV = 230 × 194 mm<sup>2</sup>, voxel size = 0.7 × 0.7 × 6.0 mm<sup>3</sup>, and matrix = 320 × 224. The MR imaging data were stored in DICOM format.

### Image Processing and Segmentation

In neuroimaging studies, the ROIs are located in the brain tissue. Therefore, we removed the nonbrain tissue in MR imaging using a deep learning model.<sup>28</sup>

ROIs of the cortical tubers and migration lines were manually drawn by 2 neuroradiologists with >15 years of experience who were blinded to clinical data using open-source software (ITK-SNAP, Version 3.8.0; <http://www.itksnap.org>). ROIs were merged when the difference between the individual ROIs determined by the 2 neuroradiologists was <5%. When there was a >5% difference between these 2 ROIs, the ROI used was determined by a senior neuroradiologist. ROIs of the cortical tubers and migration lines were defined as areas of the MR images that exhibited abnormal hyperintense or hypointense signals. Figure 2 shows some cases of FLAIR images with and without lesions and segmentation in children with TSC. Figure 2A shows the FLAIR images of some children with TSC with lesions, and Fig 2B is the segmentation of Fig 2A. Figure 2C shows the FLAIR images of some children with TSC without lesions.

### Radiomic Feature Extraction

Due to differences in equipment parameters such as layer thickness and pixel pitch of MR images, all images were resampled to 1 × 1 × 1 mm<sup>3</sup>. A publicly available Python package, pyradiomics 3.0.1 (<https://pypi.org/project/pyradiomics/>), was used to extract radiomic features.<sup>29</sup> A total of 1132 features consisting of gray-level co-occurrence matrix (GLCM), gray-level run-length matrix (GLRLM), gray-level size zone matrix (GLSZM), gray-level dependence matrix (GLDM), first-order, and shape features were extracted from ROIs on FLAIR.

First-order features described the distribution of voxel intensity within the ROI 3D matrix and the overall information about the cortical tubers. The shape features reflected the volume, surface area, and shape of the cortical tubers. GLCM, GLRLM, GLSZM, and GLDM were collectively referred to as texture

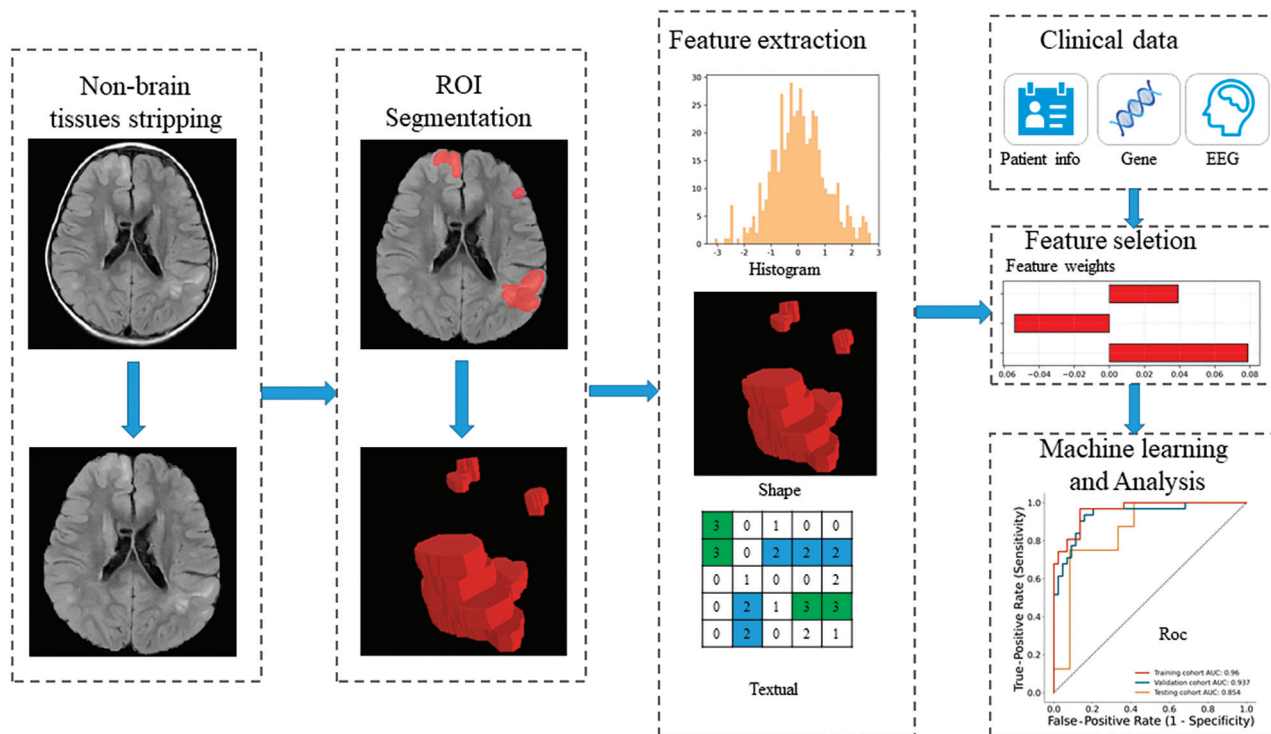


**FIG 1.** The flowchart of the current study. Patient information, including sex, age, the existence of typical symptoms of TSC, and some examination results. *TSC1* and *TSC2* were gene test results.

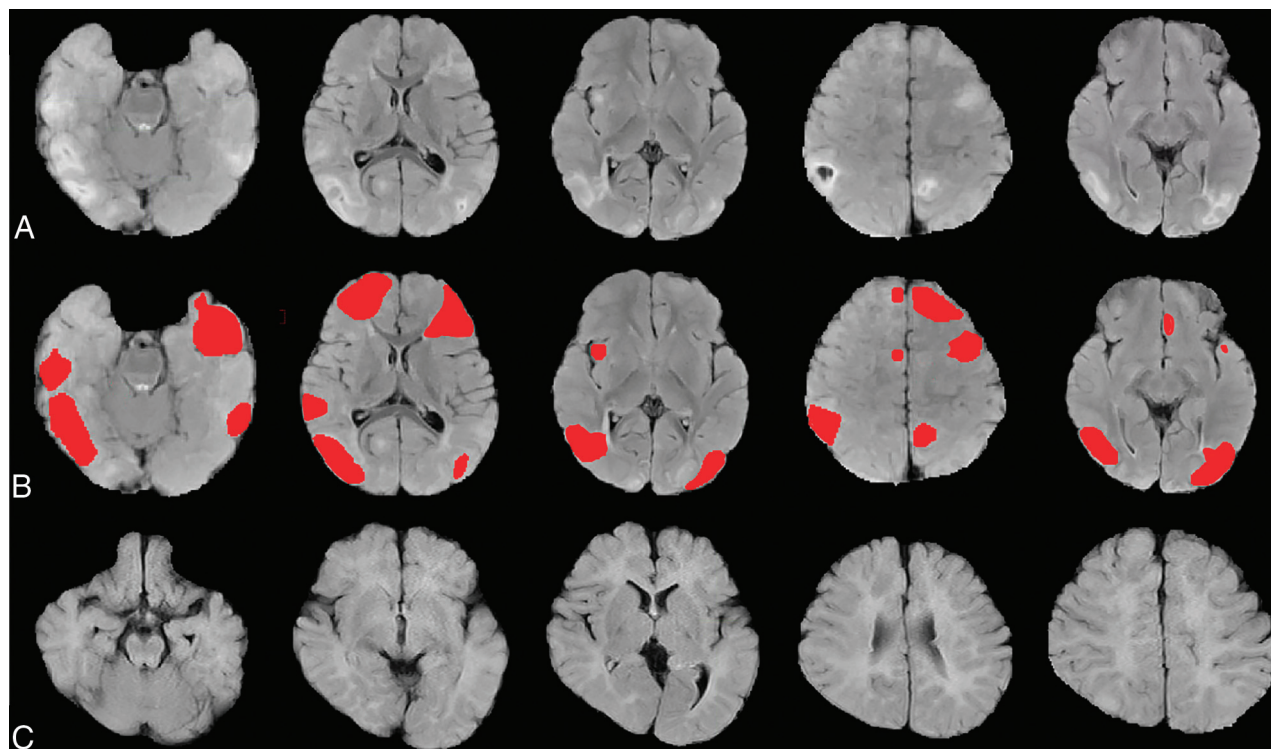


**FIG 2.** Some cases of FLAIR images with and without lesions and segmentation in children with TSC. A, The FLAIR images of some children with TSC with lesions. B, The segmentation of A. C, The FLAIR image of some children with TSC without lesions. The red color represents the segmentation of lesions.

features. The detailed information and formulas for the detection of the 1132 radiomic features are described in <https://pyradiomics.readthedocs.io/en/latest/>.

#### Feature Selection

The 1132 radiomic features and 59 routine clinical variables were normalized with *z* score normalization before feature selection.



**Table 1: The radiomic and clinical features selected by LASSO regression**

Selected Features	P Value of Spearman Correlation <sup>a</sup>	Coefficients of LASSO
Radiomic features		
log-sigma-2-0-mm-3D_gldm_SmallDependenceHighGrayLevelEmphasis	.030	0.026695
wavelet-LLH_gldm_Idmn	.036	−0.051160
wavelet-LLL_firstorder_10Percentile	.012	0.023878
wavelet-LLL_firstorder_Mean	.035	0.050790
Clinical features		
Age of onset	<.001	0.117626
Infantile spasms	<.001	−0.147036
Epileptiform discharge in left parieto-occipital area of EEG	<.001	0.098540
ASM numbers	.018	−0.132026
Gene mutation type	.025	−0.047780

First, a bivariate analysis was conducted to screen the radiomic and clinical features. We calculated the *P* values of the Spearman correlation coefficient between each feature and the treatment outcome and identified the features with *P* values < .05. Least absolute shrinkage and selection operator (LASSO) was widely used to compress the coefficients of features and select features to prevent overfitting, so we used a LASSO algorithm to select the key radiomic and clinical features.

#### Development and Evaluation of an Individualized Prediction Model

On the basis of a cohort of all patients, we used 11 machine learning classifiers, such as support vector machines, random forest, logistic regression, AdaBoost (<https://www.machinelearningplus.com/machine-learning/introduction-to-adaboost>), gradient boosting, and decision tree to build models to predict treatment outcome with clinical information and radiomic features.

Each classifier was trained on the training set using a 10-fold cross-validation procedure and the training process needed to determine the optimal hyperparameters of the classifiers, which were determined by grid search. We selected the best classifier by comparing the performance of classifiers on the validation set. The classifier that achieved the highest area under the receiver operating curve (AUC) score was selected as a candidate solution.

Once trained, the best model was evaluated on the test set. The classification performance of the model was assessed by the receiver operating characteristic curves and AUCs in each cohort. Calibration curves were also plotted to assess the calibration of the radiomic and clinical features.<sup>30</sup>

#### Statistical Analysis

In this study, we use frequencies and percentages for categorical variables and median and range for continuous variables. The differences between groups were assessed by an independent samples *t* test, and *P* < .05 was defined as significant. Model training, validation, and testing were implemented with Python (Version 3.8.0).

## RESULTS

#### Demographic and Clinical Data

The main clinical and pathologic characteristics of all 105 patients are listed in the Online Supplemental Data. Of the 105 enrolled patients, 43 (40.9%) were controlled and 62 (59.1%) were

uncontrolled by drug treatment. Age of onset, infantile spasms, gene mutation type, ASM numbers, and epileptiform discharge in the left parieto-occipital area of the EEG were significantly different between the controlled and uncontrolled patients (*P* < .05).

#### Performance of the Radiomic Signature

Four key radiomic features and 5 clinical features were selected using the Spearman correlation analysis and LASSO regression (Table 1), and the distribution of each radiomic feature in the controlled

and uncontrolled groups is shown in Fig 3A–D. According to the AUC of the validation set that was used to select the best hyperparameters and model, the best classification model is logistic regression (Fig 4). The predictive ability of the model with radiomic and clinical features was shown by the receiver operating characteristic curve (Fig 5A), achieving the best performance of AUC = 0.96, classification accuracy = 90.7%, sensitivity = 0.97, and specificity = 0.86 in the training cohort; AUC = 0.94, classification accuracy = 88.0%, sensitivity = 0.94, and specificity = 0.84 in the validation cohort; and AUC = 0.854, classification accuracy = 80.0%, sensitivity = 0.75, and specificity = 0.83 in the test cohort, respectively. Table 2 shows the test set results on logistic regression models with input of clinical features alone and with input of radiomic and clinical features. Figure 6 shows a performance comparison of clinical features alone and radiomic and clinical features on a logistic regression model in the testing cohorts. The results of the test set with the logistic regression model are shown in Table 2. The model of radiomic and clinical features demonstrated favorable calibration in the training, validation, and testing cohorts (Fig 5B). Figure 5C–E shows the waterfall plots of radiomics and the clinical model to differentiate controlled from uncontrolled patients in the training, validation, and testing cohorts.

## DISCUSSION

With the increasing use of drug treatments in epilepsy, a better understanding of patient response to the treatment could help identify the optimal treatment strategy for individual patients.<sup>10</sup> Radiomic approaches, when combined with clinical data, could improve treatment selection. In this study, a prediction model of drug treatment outcome based on radiomic data from MR imaging and clinical data was developed. The results demonstrate that the MR imaging–based radiomic and clinical models could successfully predict the outcome of epilepsy drug treatment among children with TSC.

Reliable prediction of epilepsy drug treatment outcome allows the development of a more targeted treatment, and those patients proved to be drug-resistant should be considered for surgical procedures or other treatment options to increase the curative ratio and reduce mortality.<sup>31,32</sup> However, determining the epilepsy drug treatment outcome on the basis of its clinical and treatment presentation imposes an apparent lag. Thus, there is a need for a

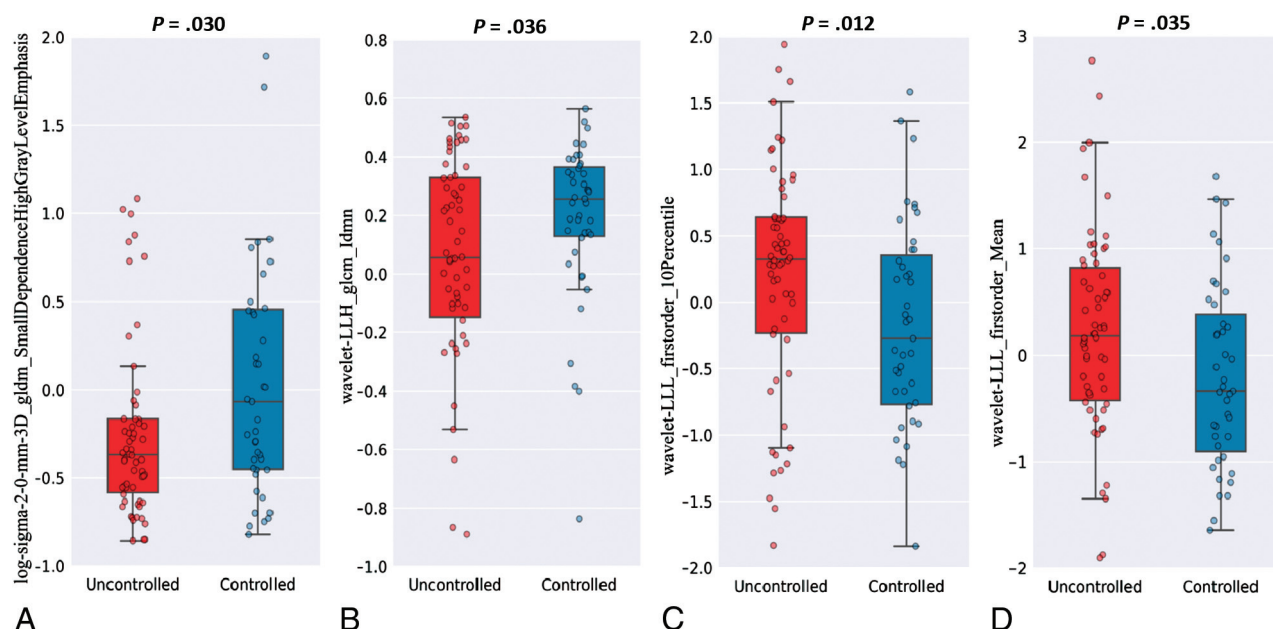


**FIG 3.** Boxplot of the 4 selected values of radiomic features in controlled and uncontrolled groups. The small *blue and red circles* represent the value of each radiomic feature in the controlled and uncontrolled groups. The *middle line* of the boxplot is the median of the radiomic feature, representing the average level of the radiomic feature. The *upper and lower bounds* of the boxplot are the upper and lower quartiles of the radiomic feature data, respectively. *P* values are the results of the Spearman correlation test.

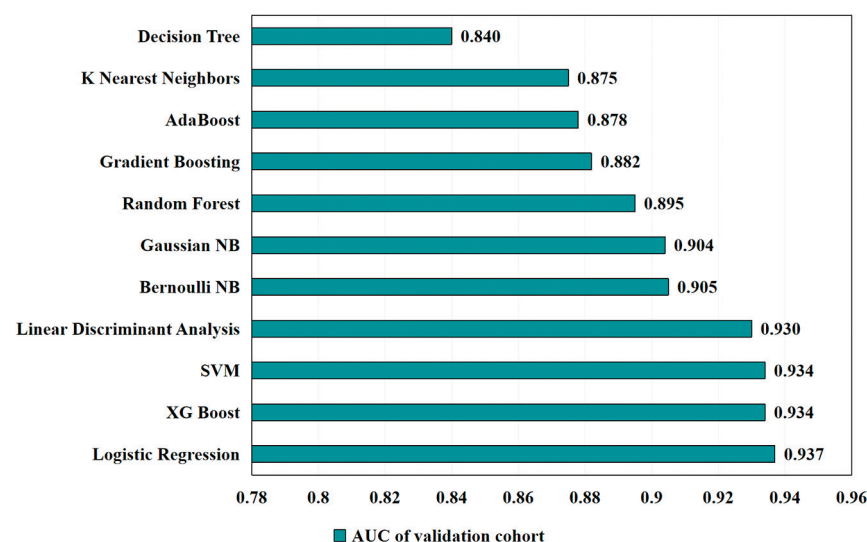


**FIG 4.** The AUC scores of 11 machine learning models in the validation cohort. According to the AUC of the validation set that was used to select the best hyperparameters and model, the best classification model of radiomic and clinical features is logistic regression. NB indicates Naive Bayes; SVM, support vector machine; XG, eXtreme Gradient.

clinical model capable of predicting epilepsy drug treatment outcome before treatment initiation. In this study, a new model with radiomic and clinical features was developed at baseline to predict the epilepsy drug treatment outcome for patients with TSC, which will provide clinicians with a reliable and noninvasive tool to better select patients for epilepsy drug treatment.

With the rapid development of machine learning and image-processing techniques, a number of studies have developed radiomics-based predictive models for various clinical characteristics, including pathologic grade<sup>33,34</sup> and treatment and survival

outcomes.<sup>35,36</sup> The rapid increase of the radiomic application is driven by enriched quantitative image features that clinicians can extract from medical images with high efficiency to guide clinical decision-making.<sup>37</sup> Moreover, some researchers have successfully applied radiomic analysis to predict tumor-related epilepsy by combining various quantitative MR imaging features.<sup>18,20-22</sup> Their works mainly focused on tumor-related epilepsy. However, epilepsy caused by TSC is different. It has distinct clinical manifestations and presentations on MR imaging.<sup>10</sup>

To our knowledge, this is the first study to show that radiomics can be used to predict the outcome of epilepsy drug treatment in patients with TSC. Therefore, we tried to demonstrate the associations of these radiomics-based MR imaging features with TSC-related

epilepsy drug treatment outcome, and we have achieved a relatively high discrimination accuracy and AUC in all cohorts, which suggest that the radiomic model developed in this study was effective in predicting the outcome of epilepsy drug treatment.

In our study, we selected 4 radiomic features to predict drug treatment outcomes, including  $\log\text{-sigma-2-0-mm-3D\_gldm\_SmallDependenceHighGrayLevelEmphasis}$  (L\_gldm\_S),  $\text{wavelet-LLH\_gldm\_Idmn}$  (W\_gldm\_I),  $\text{wavelet-LLL\_firstorder\_10Percentile}$  (W\_firstorder\_10), and  $\text{wavelet-LLL\_firstorder\_Mean}$  (W\_firstorder\_M). L\_gldm\_S and W\_gldm\_I are texture features

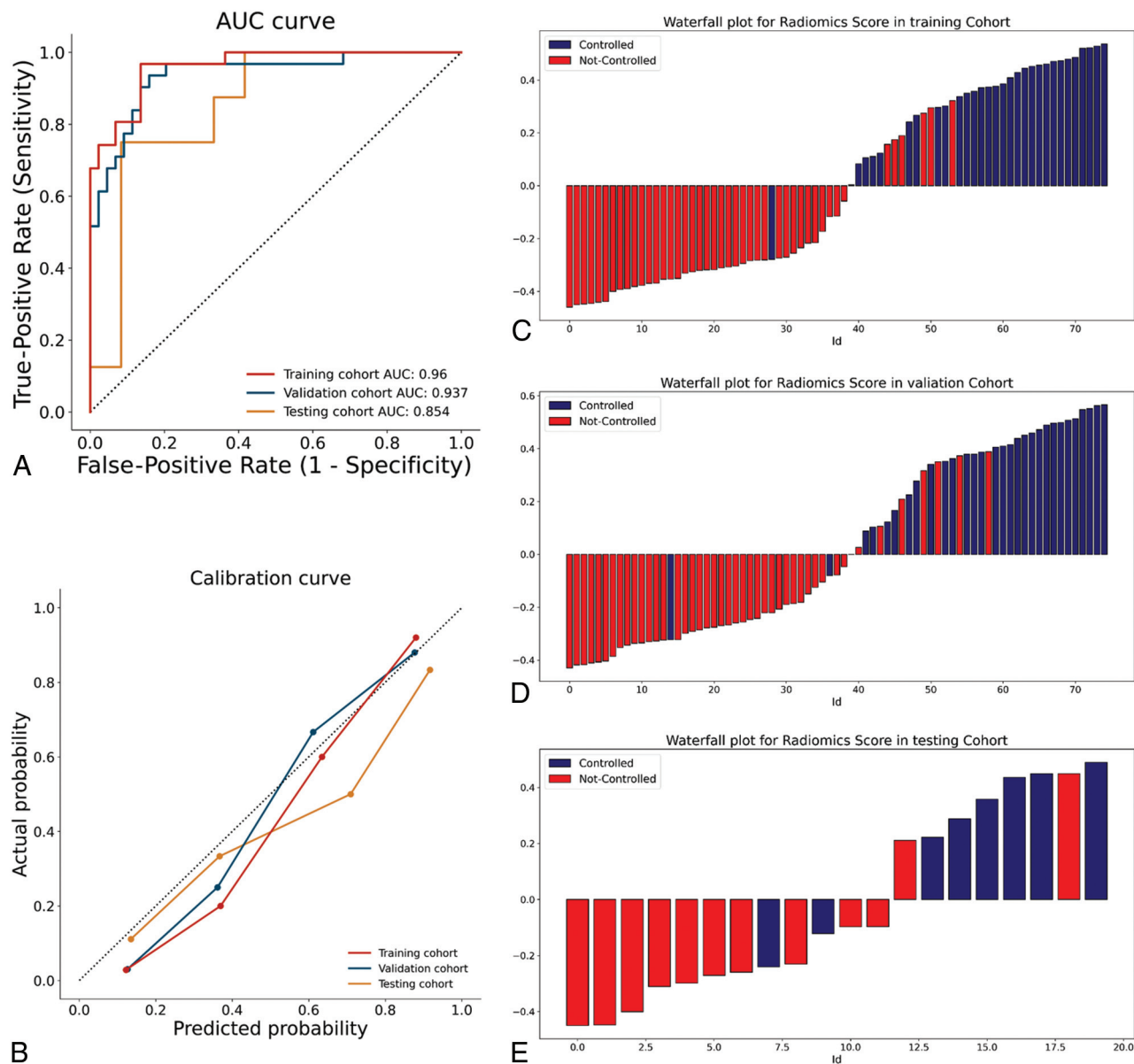


**FIG 5.** Receiver operating characteristic curve (A), calibration curve (B), and waterfall plots (C–E) of the radiomic and clinical features model in training, cross-validation, and testing cohorts.

**Table 2: The results of the logistic regression model in testing cohorts**

Input Features	Model	AUC	ACC	SEN	SPE
Clinical features	Logistic regression	0.783	0.767	0.769	0.765
Radiomic and clinical features	Logistic regression	0.854	0.800	0.750	0.830

**Note:**—ACC indicates accuracy; SEN, sensitivity; SPE, specificity.

that reflect the homogeneity of the tubers. W\_firstorder\_10 and W\_firstorder\_M are first-order statistical features that reflect the distribution of signal intensities within the tuber region. Our results imply that the texture features and first-order statistical features are valuable for predicting drug treatment outcomes. Zhao et al<sup>38</sup> had reported that the type II lesions (the uneven thickening of the cortex on T2-weighted and FLAIR) were statistically significant between the uncontrolled and controlled groups, similar to findings in our research. MR imaging lesion type features are related to outcomes of epilepsy drug treatment in TSC,<sup>10,12</sup> which can

indirectly support our present results because the types of lesions are generally classified clinically according to texture structure and the signal intensity of the lesions.

Additionally, our model incorporated both radiomic features and clinical characteristics that are helpful for prediction, such as the age of onset, infantile spasms, ASM numbers, epileptiform discharge in left parieto-occipital area of the EEG, and gene mutation type, making our model more comprehensive and reliable for clinical application. Our study found that about 59.1% of patients with TSC were in the uncontrolled group. It was reported that the drug resistance ratios of TSC-related epilepsy were 59.6%,<sup>38</sup> 60%,<sup>5</sup> and 62%,<sup>39</sup> which were similar to those in our study. In addition, about 30 (48.4%) patients in the uncontrolled group had experienced infantile spasms, and 4 (9.3%) patients in the

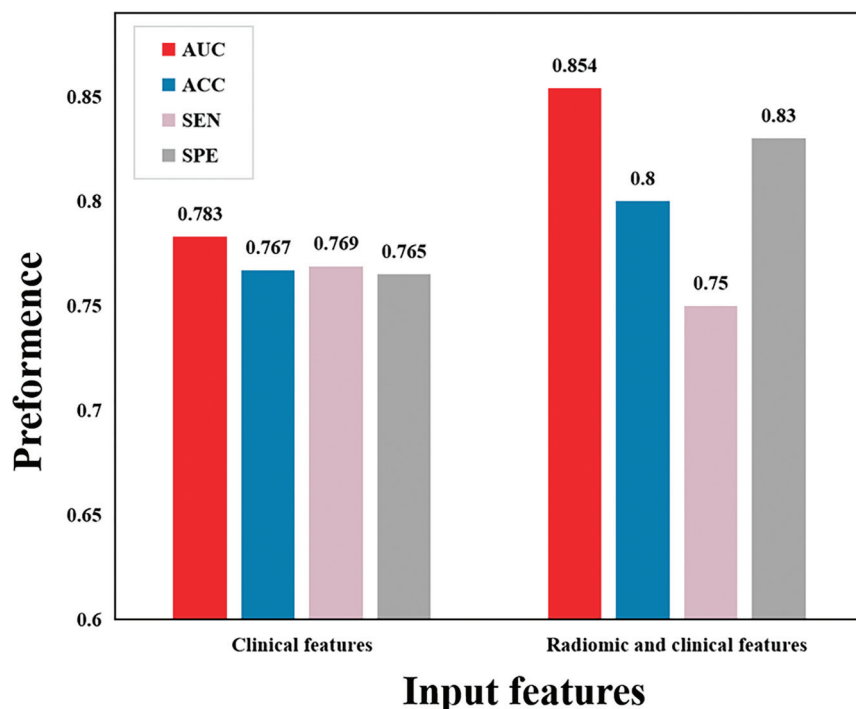


**FIG 6.** The performance comparison of clinical features alone and radiomic and clinical features on a logistic regression model in testing cohorts. ACC indicates accuracy; SEN, Sensitivity; SPE, specificity.

controlled group had experienced infantile spasms. Previous studies have shown similar results: TSC patients with infantile spasms are more likely to develop drug resistant epilepsy.<sup>4,40</sup> In our study, the mean age of seizure onset was 10.34 months in the uncontrolled group and 31.17 months in the controlled group. Patients with TSC epilepsy before 1 year of age are more likely to develop resistance than those with onset after 1 year of age,<sup>40</sup> consistent with our results. Compared with *TSC1* pathogenic mutations, *TSC2* mutations have a more severe clinical phenotype, and the conditions of these patients are usually more difficult to control,<sup>39,41</sup> consistent with our findings that the proportion of *TSC2* gene mutations was higher in the uncontrolled group.

Our results showed that the severity of EEG discharge in the left parieto-occipital area was correlated with the epilepsy drug treatment outcome, and the EEG discharge in the uncontrolled group was more serious. Previous reports also showed similar results. Some patients with TSC with severe EEG discharges have multifocal EEG discharges related to bilateral asymmetric spike-and-wave complexes. The onset is partial seizures or convulsive seizures, which later develop into drug-resistant epilepsy.<sup>39,40</sup> In a study of 83 patients with TSC, ASM numbers have been reported as an important risk factor for development of refractory epilepsy in patients with TSC.<sup>6</sup> In our study, the history of using >3 ASMs is the risk factor that will lead to occurrence of drug-resistant epilepsy.

LASSO is a widely accepted algorithm in feature selection. The 1132 radiomics features extracted in this study may cause overfitting when constructing the model. Therefore, feature dimension reduction and selection were performed to screen the key features that are most closely related to the epilepsy drug

treatment outcome using bivariate analysis and the LASSO algorithm. With features associated with epilepsy drug treatment outcome, we used 11 classic machine learning models for classification and selected the best model on the basis of AUC of cross-validation. Finally, we evaluated the performance of the selected model on the independent test set consisting of unseen data.

Although this study is novel and conducted with advanced methodology, there are several limitations. First, it is a single-center cohort study, and a multi-center cohort study should be further considered to verify the findings of this study. Second, the data set is relatively small because TSC is a rare disease. However, we will collect more data from additional patients with TSC and will use advanced algorithms such as deep learning to make more precise predictions in the future. Finally, our study used only the MR imaging technique, which contains limited information. We will explore the multimodal data such as

CT and PET to construct a more comprehensive radiomic model in future exploration.

## CONCLUSIONS

Our study suggests that radiomics could be a noninvasive, efficient, and reliable way to predict patient outcome to drug treatment when combined with clinical data. Furthermore, we identified novel models containing informative clinical covariates and radiomic image features to predict drug treatment outcome. Our results implied that the texture features and first-order statistics features are the most valuable radiomic features for predicting drug treatment outcomes. Age of onset, infantile spasms, ASM numbers, epileptiform discharge in the left parieto-occipital area of EEG, and gene mutation type are the key clinical factors that are most likely to predict the epilepsy drug treatment outcome.

Disclosure forms provided by the authors are available with the full text and PDF of this article at [www.ajnr.org](http://www.ajnr.org).

## REFERENCES

1. Randle SC. **Tuberous sclerosis complex: a review.** *Pediatr Ann* 2017;46:e166–71 [CrossRef Medline](#)
2. Henske EP, Jóźwiak S, Kingswood JC, et al. **Tuberous sclerosis complex.** *Nat Rev Dis Primers* 2016;2:16035 [CrossRef Medline](#)
3. Curatolo P, Nabbout R, Lagae L, et al. **Management of epilepsy associated with tuberous sclerosis complex: updated clinical recommendations.** *Eur J Paediatr Neurol* 2018;22:738–48 [CrossRef Medline](#)
4. Słowińska M, Jóźwiak S, Peron A, et al. **Early diagnosis of tuberous sclerosis complex: a race against time: how to make the diagnosis before seizures?** *Orphanet J Rare Dis* 2018;13:25 [CrossRef Medline](#)



5. Fohlen M, Taussig D, Ferrand-Sorbets S, et al. **Refractory epilepsy in preschool children with tuberous sclerosis complex: early surgical treatment and outcome.** *Seizure* 2018;60:71–79 [CrossRef Medline](#)
6. Gül Mert G, Altunbaşak Ş, Hergüner Ö, et al. **Factors affecting epilepsy prognosis in patients with tuberous sclerosis.** *Childs Nerv Syst* 2019;35:463–68 [CrossRef Medline](#)
7. van der Poest Clement E, Jansen FE, Braun KP, et al. **Update on drug management of refractory epilepsy in tuberous sclerosis complex.** *Paediatr Drugs* 2020;22:73–84 [CrossRef Medline](#)
8. Jóźwiak S, Kotulska K, Domańska-Pakieła D, et al. **Antiepileptic treatment before the onset of seizures reduces epilepsy severity and risk of mental retardation in infants with tuberous sclerosis complex.** *Eur J Paediatr Neurol* 2011;15:424–31 [CrossRef Medline](#)
9. Jesmanas S, Norvainytė K, Gleiznienė R, et al. **Different MRI-defined tuber types in tuberous sclerosis complex: quantitative evaluation and association with disease manifestations.** *Brain Dev* 2018;40:196–204 [CrossRef Medline](#)
10. Yang J, Zhao C, Su S, et al. **Machine learning in epilepsy drug treatment outcome prediction using multi-modality data in children with tuberous sclerosis complex.** In: *Proceedings of the 2020 6th International Conference on Big Data and Information Analytics (BigDIA)*, Shenzhen, China; December 4–6, 2020
11. Russo C, Nastro A, Cicala D, et al. **Neuroimaging in tuberous sclerosis complex.** *Childs Nerv Syst* 2020;36:2497–509 [CrossRef Medline](#)
12. Grilli G, Moffa AP, Perfetto F, et al. **Neuroimaging features of tuberous sclerosis complex and Chiari type I malformation: a rare association.** *J Pediatr Neurosci* 2018;13:224–28 [CrossRef Medline](#)
13. Hulshof HM, Benova B, Krsek P, et al. **The epileptogenic zone in children with tuberous sclerosis complex is characterized by prominent features of focal cortical dysplasia.** *Epilepsia Open* 2021;6:663–71 [CrossRef Medline](#)
14. Stafstrom CE, Staedtke V, Comi AM. **Epilepsy mechanisms in neurocutaneous disorders: tuberous sclerosis complex, neurofibromatosis type 1, and Sturge-Weber syndrome.** *Front Neurol* 2017;8:87 [CrossRef Medline](#)
15. Mayerhoefer ME, Materka A, Langs G, et al. **Introduction to radiomics.** *J Nucl Med* 2020;61:488–95 [CrossRef Medline](#)
16. Yip SS, Aerts HJ. **Applications and limitations of radiomics.** *Phys Med Biol* 2016;61:R150–66 [CrossRef Medline](#)
17. Rizzo S, Botta F, Raimondi S, et al. **Radiomics: the facts and the challenges of image analysis.** *Eur Radiol Exp* 2018;2:36 [CrossRef Medline](#)
18. Liu Z, Wang Y, Liu X, et al. **Radiomics analysis allows for precise prediction of epilepsy in patients with low-grade gliomas.** *Neuroimage Clin* 2018;19:271–78 [CrossRef Medline](#)
19. Park YW, Choi YS, Kim SE, et al. **Radiomics features of hippocampal regions in magnetic resonance imaging can differentiate medial temporal lobe epilepsy patients from healthy controls.** *Sci Rep* 2020;10:19567 [CrossRef Medline](#)
20. Sun K, Liu Z, Li Y, et al. **Radiomics analysis of postoperative epilepsy seizures in low-grade gliomas using preoperative MR images.** *Front Oncol* 2020;10:1096 [CrossRef Medline](#)
21. Wang Y, Wei W, Liu Z, et al. **Predicting the type of tumor-related epilepsy in patients with low-grade gliomas: a radiomics study.** *Front Oncol* 2020;10:235 [CrossRef Medline](#)
22. Zhang Y, Yan P, Liang F, et al. **Predictors of epilepsy presentation in unruptured brain arteriovenous malformations: a quantitative evaluation of location and radiomics features on T2-weighted imaging.** *World Neurosurg* 2019;125:e1008–15 [CrossRef Medline](#)
23. He B, Dong D, She Y, et al. **Predicting response to immunotherapy in advanced non-small-cell lung cancer using tumor mutational burden radiomic biomarker.** *J Immunother Cancer* 2020;8:e000550 [CrossRef Medline](#)
24. Khorrami M, Prasanna P, Gupta A, et al. **Changes in CT radiomic features associated with lymphocyte distribution predict overall survival and response to immunotherapy in non-small cell lung cancer.** *Cancer Immunol Res* 2020;8:108–19 [CrossRef Medline](#)
25. Sun R, Limkin EJ, Vakalopoulou M, et al. **A radiomics approach to assess tumour-infiltrating CD8 cells and response to anti-PD-1 or anti-PD-L1 immunotherapy: an imaging biomarker, retrospective multicohort study.** *Lancet Oncol* 2018;19:1180–91 [CrossRef Medline](#)
26. Trebeschi S, Drago SG, Birkbak NJ, et al. **Predicting response to cancer immunotherapy using noninvasive radiomic biomarkers.** *Ann Oncol* 2019;30:998–1004 [CrossRef Medline](#)
27. Tunali I, Gray JE, Qi J, et al. **Novel clinical and radiomic predictors of rapid disease progression phenotypes among lung cancer patients treated with immunotherapy: an early report.** *Lung Cancer* 2019;129:75–79 [CrossRef Medline](#)
28. Isensee F, Schell M, Pflueger I, et al. **Automated brain extraction of multisequence MRI using artificial neural networks.** *Hum Brain Mapp* 2019;40:4952–64 [CrossRef Medline](#)
29. van Griethuysen JJ, Fedorov A, Parmar C, et al. **Computational radiomics system to decode the radiographic phenotype.** *Cancer Res* 2017;77:e104–07 [CrossRef Medline](#)
30. Austin PC, Harrell FE Jr, van Klaveren D. **Graphical calibration curves and the integrated calibration index (ICI) for survival models.** *Stat Med* 2020;39:2714–42 [CrossRef Medline](#)
31. Hsieh DT, Jennesson MM, Thiele EA. **Epileptic spasms in tuberous sclerosis complex.** *Epilepsy Res* 2013;106:200–10 [CrossRef Medline](#)
32. Liu S, Yu T, Guan Y, et al. **Resective epilepsy surgery in tuberous sclerosis complex: a nationwide multicentre retrospective study from China.** *Brain* 2020;143:570–81 [CrossRef Medline](#)
33. Zhang G, Xu L, Zhao L, et al. **CT-based radiomics to predict the pathological grade of bladder cancer.** *Eur Radiol* 2020;30:6749–56 [CrossRef Medline](#)
34. Mao B, Zhang L, Ning P, et al. **Preoperative prediction for pathological grade of hepatocellular carcinoma via machine learning-based radiomics.** *Eur Radiol* 2020;30:6924–32 [CrossRef Medline](#)
35. Jiang Y, Chen C, Xie J, et al. **Radiomics signature of computed tomography imaging for prediction of survival and chemotherapeutic benefits in gastric cancer.** *EBioMedicine* 2018;36:171–82 [CrossRef Medline](#)
36. Staal FC, van der Reijnd DJ, Taghavi M, et al. **Radiomics for the prediction of treatment outcome and survival in patients with colorectal cancer: a systematic review.** *Clin Colorectal Cancer* 2021;20:52–71 [CrossRef Medline](#)
37. Lambin P, Leijenaar RT, Deist TM, et al. **Radiomics: the bridge between medical imaging and personalized medicine.** *Nat Rev Clin Oncol* 2017;14:749–62 [CrossRef Medline](#)
38. Zhao X, Jiang D, Hu Z, et al. **Machine learning and statistic analysis to predict drug treatment outcome in pediatric epilepsy patients with tuberous sclerosis complex.** *Epilepsy Res* 2022;188:107040 [CrossRef Medline](#)
39. Jeong A, Nakagawa JA, Wong M. **Predictors of drug-resistant epilepsy in tuberous sclerosis complex.** *J Child Neurol* 2017;32:1092–98 [CrossRef Medline](#)
40. Chu-Shore CJ, Major P, Camposano S, et al. **The natural history of epilepsy in tuberous sclerosis complex.** *Epilepsia* 2010;51:1236–41 [CrossRef Medline](#)
41. Salussolia CL, Klonowska K, Kwiatkowski DJ, et al. **Genetic etiologies, diagnosis, and treatment of tuberous sclerosis complex.** *Annu Rev Genomics Hum Genet* 2019;20:217–40 [CrossRef Medline](#)